## ORIGINAL ARTICLE

# Adsorption removal of roxarsone, arsenite(III), and arsenate(V) using iron-modified sorghum straw biochar and its kinetics

Shuyan Zang[1] · Yingying Zuo[2] · Juan Wang[2] · Xiuming Liu[3] · Mario Alberto Gomez[2] · Lan Wei[2]

**Abstract** Arsenic (As) contamination in groundwater is a major problem in many countries, which causes serious health issues. In this paper, a novel method has been developed for the simultaneous removal of ROX and As(III/V) using the modified sorghum straw biochar (MSSB). The MSSB was characterized by X-ray diffraction, scanning electron microscopy, Fourier Transform Infrared, and Brunauer–Emmet–Teller (BET) surface area. The removal performance of MSSB for ROX, arsenite [As(III)], and arsenate (As(V)) was investigated using batch experiments. At pH of 5, the arsenic concentration of 1.0 mg/L, adsorbent dose of 1.0 g/L, the maximum adsorption capacities of ROX, As(III), and As(V) were 12.4, 5.3, and 23.0 mg/g, respectively. The adsorption behaviors were fit well with the Langmuir and the pseudo-second-order rate model. The results showed that MSSB acted as a highly effective adsorbent to simultaneously remove the composite pollution system consisted of ROX and As(III/V) in aqueous solutions, providing a promising method in environmental restoration applications.

**Keywords** Roxarsone · Arsenic · Arsenate · Sorghum straw biochar · Adsorption

✉ Juan Wang
  wangjuanlnsyuct@163.com

✉ Xiuming Liu
  lxmzkydhs@163.com

  Shuyan Zang
  zangshuyan@126.com

[1] Liaoning Engineering Research Center for Treatment and Recycling of Industrially Discharged Heavy Metals, Shenyang University of Chemical Technology, Shenyang 110142, China

[2] Shenyang University of Chemical Technology, Shenyang 110142, China

[3] State Key Laboratory of Environmental Geochemistry, Institute of Geochemistry, Chinese Academy of Sciences, Guiyang 550081, China

## 1 Introduction

Arsenic (As) is a persistent, bio-accumulative, toxic element widely distributed in the environment that has been introduced into water or soil by anthropogenic sources (Hao et al. 2018; Asere et al. 2019), such as mining of arsenic-bearing deposits, discharging of arsenic-containing wastewater, and using of arsenic-containing additives (Yasinta et al. 2018; Ali et al. 2019; Ng et al. 2004). The poisoning effect of arsenic-contaminated drinking water on human health has become more cataclysmic than any other natural catastrophe. Long-term exposure to arsenic-contaminated drinking water even at low levels of exposure, will lead to potential human health hazards, including skin cancer, stomach cancer, respiratory tract cancer, and extensive liver damage (Eisler 2004; Mohanty 2017). In natural waters, arsenic exists in both inorganic and organic forms. Inorganic arsenic is mostly found with trivalent and pentavalent states, known as As(III) and As(V), respectively (Pokhrel and Viraraghavan 2006). As one of the organic arsenic forms, roxarsone (4-hydroxy-3-nitrobenzene arsonic acid, ROX) is used as animal feeding additives for effectively preventing parasitic diseases of poultry. Previous studies indicated that a considerable amount of ROX without metabolization in animals might be released from poultry litter to soil and water (Frensemeier et al. 2017; Mahaninia and Wilson 2017; Ji et al. 2016; Guzmán-Fierro et al. 2015), which could produce

inorganic forms of arsenic, such as As(III) and As(V), displaying even higher toxicity. The mixture of arsenic compounds including both inorganic and organic arsenicals caused environmental contamination (Danish et al. 2013). The World Health Organization has been set the standard for arsenic maximum contaminant levels from 50 to 10 μg/L since 1993 (WHO 2001). To meet stringent drinking water standards, cost-effective arsenic removal technology is urgently needed.

To remove arsenic from the environment, many effective approaches have been developed, such as adsorption (Chandra et al. 2010), chemical coagulation-precipitation (Pal et al. 2007), ion-exchange (Kim and Benjamin 2004), membrane separation (Seidel et al. 2001) and biological treatments (Setyono and Valiyaveettil 2014; Wang et al. 2019). Among these methods, adsorption has been used extensively due to its low cost, high removal rate, and relatively mature application (Danish et al. 2013). Low-solubility solid materials with large specific surface area and porous structure have mainly served as adsorbents. These adsorbents can provide enough adsorption sites to combine with the pollutants in wastewater (Tian et al. 2017; Zhang and Liu 2019) for achieving sufficient control of the water pollution. Biochar (Ocinski et al. 2016; Ebrahimi et al. 2013; Tian et al. 2011; Cheraghi et al. 2014) has been commonly used as adsorbents for their advantages, such as large surface area, high stability, the low release of contaminants, recyclability, and inexpensive (Setyono and Valiyaveettil 2014). As one of the primary agricultural wastes with abundant yield, straw is usually discarded or burned directly in the field, leading to environmental pollution. Via the straw convention into bio-carbon for use as bio-sorbents or adsorbents, is a potentially efficient way to re-use and recycle this type of agricultural waste (Cheraghi et al. 2014).

For the high affinity of arsenic to iron, different iron-loaded sorbents have been made (Iglesias et al. 2013; Solesardans et al. 2016; Calugaru et al. 2019). The solid phases loaded with Fe species would promote the adsorption of arsenates and arsenites and further transformation into stable complexes (Dupont et al. 2007). In the practical applications, a series of effective approaches to improve the adsorption capacity of the adsorbent has been reported, in which the adsorbents were modified by sintering or doping with different metal ions (Philippova et al. 2011; Hossain et al. 2016; Ma et al. 2015; Su et al. 2017). To date, several methods have been reported in the literature about the single adsorption of inorganic arsenic(III, V) or ROX (Kumari et al. 2005; Dixit et al. 2003, Ustinov and Do 2002; Li et al. 2016; Yu et al. 2020), however, it is still lacking studies on the simultaneous adsorption of inorganic and organic arsenic (Fu et al. 2020).

In this paper, iron-modified bio-materials were prepared with sorghum straw biochar. And then, the materials were used to remove inorganic and organic arsenic from synthetic aqueous solutions. The results demonstrated that the as-prepared materials possessed the capability for simultaneous removal of both ROX and As(III/V). Moreover, the use of straw can reduce the cost of removal toxin and provide a promising approach for large-scale use in future applications. The adsorption process of ROX and As(III/V) on the modified sorghum straw biochar was further investigated in this paper, including adsorption kinetics, isotherms, and effects of various experimental parameters, which may provide a potential solution to the ROX and As(III/V) contaminated wastewater.

## 2 Material and methods

### 2.1 Materials

The chemical reagents used in this work $CH_3OH$ and $KH_2PO_4$ were spectrum pure and the others were analytical grade. The fresh arsenic working solutions were prepared by diluting the stock arsenate solutions with deionized water.
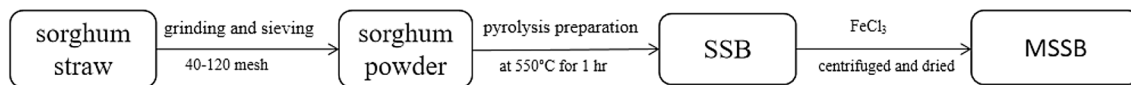
The sorghum straw biochar was prepared by pyrolysis of sorghum powder with particles size ranging from 40 to 120 mesh under an oxygen-limited condition at 550 °C for 1 h. Using X-Ray Fluorescence Spectrometer (XRF, ZSX Primus II) to test the chemical composition of sorghum straw biochar, the results were shown in Table 1. The pH of the solution was adjusted via NaOH and HCl. 5 g of sorghum straw biochar was put into 100 mL $FeCl_3$ solution with a concentration of 0.05 M, and then the mixtures were ultrasonically dispersed for 30 min and stirred for 24 h. The as-obtained solids were washed with deionized water and dried at 60 °C for 12 h. At last, the modified sorghum straw biochar (MSSB) was obtained. The flow chart of absorbents is shown in Fig. 1.

### 2.2 Batch adsorption experiments

To investigate the adsorption ability of MSSB for mixed arsenic pollutants, batch experiments were carried out. At room temperature, to adsorb arsenic, the pH value of the solution was adjusted with NaOH/HCl, then 0.1 g of MSSB was added to 100 mL mixed solution with 1 mg/L ROX and As(III/V). The adsorption performances of the adsorbent were measured by the removal rate of ROX and As(III/V). In particular, the removal rate of ROX and As(III/V) was characterized by the initial concentration and the final concentration of arsenic in the solution.

**Table 1** XRF analysis data

| Element as oxide | SiO$_2$ | Al$_2$O$_3$ | P$_2$O$_5$ | Na$_2$O | K$_2$O | Fe$_2$O$_3$ | Other |
|---|---|---|---|---|---|---|---|
| Percentage (wt%) | 50.745 | 24.277 | 23.888 | 0.307 | 0.250 | 0.211 | 0.322 |

sorghum straw → (grinding and sieving 40-120 mesh) → sorghum powder → (pyrolysis preparation at 550°C for 1 hr) → SSB → (FeCl$_3$ centrifuged and dried) → MSSB

**Fig. 1** The flow chart of MSSB

### 2.2.1 Arsenic adsorption edges

To investigate the effect of pH value on the adsorption of arsenic by the adsorbent, the batch experiments were conducted at different pH values (from 1.0 to 11.0) by adding NaOH or HCl solution.

### 2.2.2 Adsorption kinetics

The adsorption equilibrium time was determined by the batch experiments. 0.1 g adsorbent was put into a 100 mL with the concentration of ROX and As(III/V) of 1.0 mg/L, and then the mixture was shaken on a platform shaker (150 rpm) at pH = 5.0 for different reaction times. The selected reaction time intervals were 0.083, 0.25, 0.5, 1, 4, 8, 12, 24, 30, 36 and 48 h. To measure the concentrations of As, about 1 mL mixture was removed from the vessel at different reaction times, then filtered with a 0.22 μm filter.

The removal rate (R, %) and the removal capacity (Q$_e$, mg/g) of ROX and As(III/V) were calculated using the following equations (Feng et al. 2019):

$$Qe = \frac{(C0 - Ce) \cdot V}{m} \quad (1)$$

$$R(\%) = \frac{(C0 - Ce)}{C0} \cdot 100 \quad (2)$$

where $C_0$ and $C_e$ are the initial and equilibrium concentrations of ROX and As (III/V), V is the solution volume (L), and m is the mass of the adsorbent (g).

### 2.2.3 Arsenic adsorption isotherms

To estimate the maximum adsorption capacity of the adsorbent, the adsorption isotherms of MSSB were conducted. The adsorption tests were carried out for the mixed solutions with different initial concentrations C$_0$ (0.1, 1.0, 10, 20, 50 mg/L) of ROX and As(III/V), respectively, and the pH value of the solution was 5.0. Then, 0.1 g absorbent was added to each solution and shaken on an orbit shaker at 150 rpm for 48 h. The Langmuir, Freundlich, and Dubinin-Radushkevich isotherms based on the data were obtained from the above experiments under the optimal conditions.

### 2.2.4 Analytical methods

As(V) was initially reduced to As(III) by thiourea and ascorbic acid (5 g thiourea and 5 g ascorbic acid in 100 mL H$_2$O), and then Atomic Fluorescence Spectrophotometer (AFS-HG Hydride generation, AFS-2202E) was used to determine the amount of As(III) in solution. The total inorganic arsenic content was determined by AFS-HG and the concentration of As(V) was calculated by subtraction (Guo et al. 2011).

High-performance liquid chromatography (HPLC, Primaide1210) with a C18 reversed-phase column was used to determine the concentration of ROX. The mobile phase was 15% CH$_3$OH and 85% KH$_2$PO$_4$ (V/V) buffer solution, the pH value was 3.0, the elution time was 8 min, the detection wavelength was 266 nm and the flow rate was 2.0 mL·min$^{-1}$.

The phase and morphology of the adsorbent were characterized by X-ray diffraction (XRD, D8 Quest), Fourier Transform Infrared (FTIR, NICOLET6700), and scanning electron microscopy (SEM, JSM-636OLV). The surface area of the materials was determined by Brunauer–Emmett–Teller (BET) method. The pore size distribution and total volume were calculated by the Brunauer-Joyner-Hallenda (BJH) method applied to the desorption data.

The point of zero charge (pH$_{PZC}$) of adsorbents was estimated according to the method described by Wang et al. (2019). In detail, the adsorbents were first suspended in 0.01 M NaCl until the pH value remained stable. Then, the pH of the suspension was adjusted to different values between 3 and 9 by adding NaOH or HCl. After equilibration for 2 h, the initial pH was recorded. Then, 1.5 g NaCl was added into each suspension and the final pH was measured after 3 h. The pH$_{PZC}$ was identified as the point at which the ΔpH is equal to 0 in the curve of ΔpH vs. the final pH. ΔpH was calculated by the difference between the final pH and the initial pH.

# 3 Results and discussion

## 3.1 Characterization and evaluation of the adsorbent

To analyze the possible adsorption mechanism of ROX and As(III/V) on the adsorbents, the morphology of SSB and MSSB was investigated firstly.

The SEM images of two absorbents are shown in Fig. 2. As shown in Fig. 2, the particles of SSB exhibited irregular shapes with smooth surfaces. After modification with FeCl₃, the surface of the adsorbent became rough and uneven. It may be attributed to the surface that was saturated with other particles, such as iron(III)-oxy or hydroxides. The BET measurements showed that the specific surface area of the absorbent was 43.39 m²/g after Fe-modification. After simultaneous adsorption of ROX and As(III/V), the surface of MSSB became rougher, indicating many small particles adhered to the adsorbent surface. The effect may be due to the pores on the adsorbent surface occupied with arsenic ions through complex physical and chemical reactions. The XRD patterns of the MSSB before and after As adsorption are shown in Fig. 3. The main peaks of the MSSB before and after As adsorption were assigned to SiO₂. Furthermore, crystal phases of iron(III)-oxy/hydroxides and As were undetected, indicating that As and iron likely existed in amorphous forms on MSSB (Zhu et al. 2020).

FTIR analysis of the samples was conducted and the results are shown in Fig. 4. The FTIR spectra of the samples were generally similar, indicating that the molecular structure of the straw biochar remained unchanged after modification and absorption, besides the appearance of a carbonyl band. The broad peak at 3386 cm$^{-1}$ in the SSB corresponds to OH/H₂O group and shifted to 3428 cm$^{-1}$ after modification. The shift towards lower wavenumbers for OH/H₂O groups in MSSA may be attributed to the
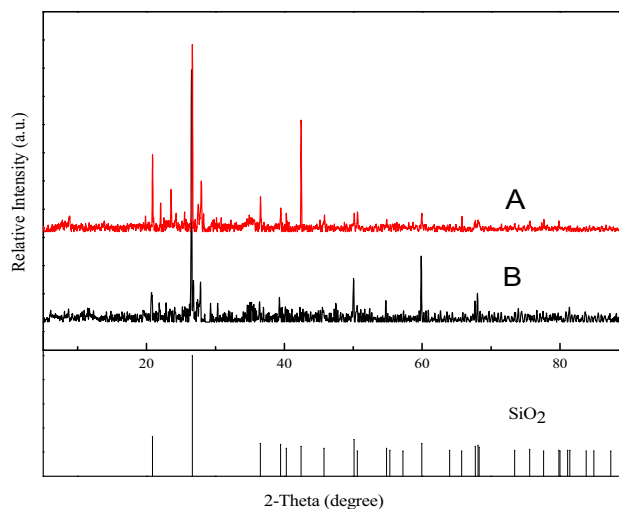


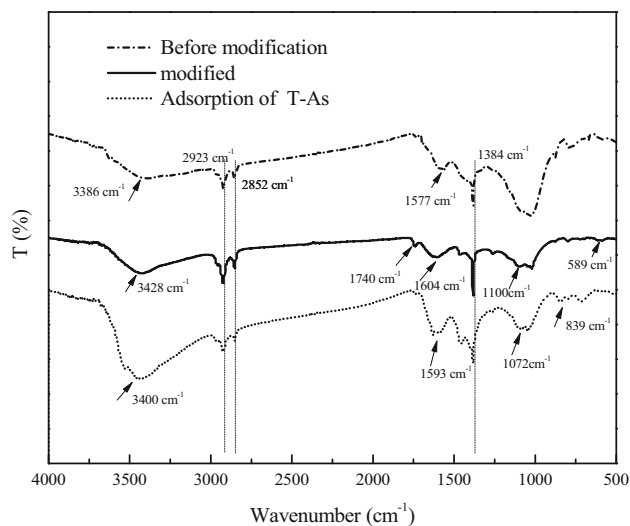Fig. 3 XRD of MSSB (**a**) and MSSB after adsorbed by As (**b**)



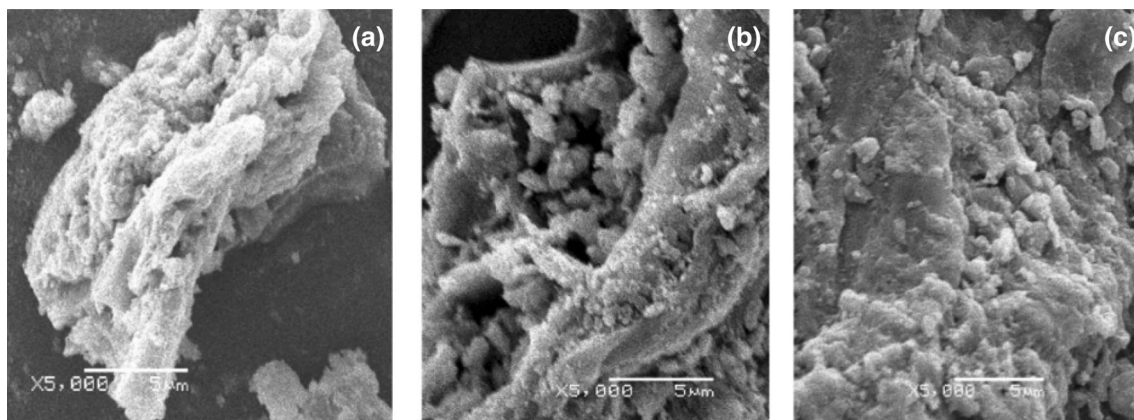Fig. 4 FTIR spectra of sorghum straw biochar



Fig. 2 SEM of SSB (**a**), MSSB (**b**), and MSSB after adsorbed by As (**c**)

stronger H-bonding that occurs and/or as a result of contributing effects from the amorphous Fe(III)-oxy/hydroxides formed (Lee et al. 2010; Gomez et al. 2011). It has been reported that large numbers of OH groups in the cellulose on the surface of straw (Ustinov and Do 2002) are beneficial to the adsorption of ROX and As(III/V) for the highly attractive to arsenic ions in solution (Ustinov and Do 2002). After adsorption, the OH/$H_2O$ on the MSSB changed in relative intensely of well shifted to high wavenumbers, indicating some type of interaction occurred between As and the functional groups of MSSB. An additional band at 3550 $cm^{-1}$ implies the additional type of H-bonding interactions occurred in the adsorption process (Lee et al. 2010; Gomez et al. 2011). It is worth noting that after modification, a new band occurred in the MSSB at ~ 1740 $cm^{-1}$ which could be contributing to C=O groups (Gomez et al. 2011) but disappeared after adsorption. It possibly indicated that the MSSB containing carboxylate groups or similar functional groups was beneficial to absorb ROX and As(III/V) (Lee et al. 2010). The vibrational band at 1577 $cm^{-1}$ corresponds to the C = C species in the SSB and shifted towards higher energy (1604 $cm^{-1}$) after modification which may indicate that groups were strained (Hu et al. 2012). After adsorption, a red-shift occurred for these vibrational bands, and the vibrational strength decreased, demonstrating that these groups served as functional adsorption sites of arsenic and could enhance the adsorption ability of arsenic from a solution compared with the previous research (Ansone et al. 2013). However, as we have observed here carbonyl and carboxylate groups may also be involved in the adsorption of arsenic. Furthermore, a band at 589 $cm^{-1}$ corresponding to the Fe–O stretch vibration (Yang et al. 2016) was observed in MSSB, indicating a Fe(III)-oxy/hydroxide was formed on the adsorbent (Lin et al. 2019). After adsorption, a new peak at 839 $cm^{-1}$ corresponded to As-O stretching shows that As was successfully adsorbed on the surface of the adsorbent (Xie et al. 2019). Therefore, based on the vibrational data, the functional groups of OH, C=C, C=O, C–O, and Fe–O on the MSSB may play important roles in effectively binding arsenic from solution.

## 3.2 Adsorbent performance evaluation

To evaluate the adsorption effect of SSB and MSSB, the removal rates of ROX and As(III/V) in the aqueous system were conducted and the results were shown in Fig. 5. From Fig. 5, the removal rates of ROX, As(III), and As(V) with the SSB respectively were 18.06%, 12.87%, and 34.66%, but they were improved significantly to 70.56%, 51.66%, and 95.96% by using the MSSB. The significant increase in adsorbing ability of MSSB may be attributed to two
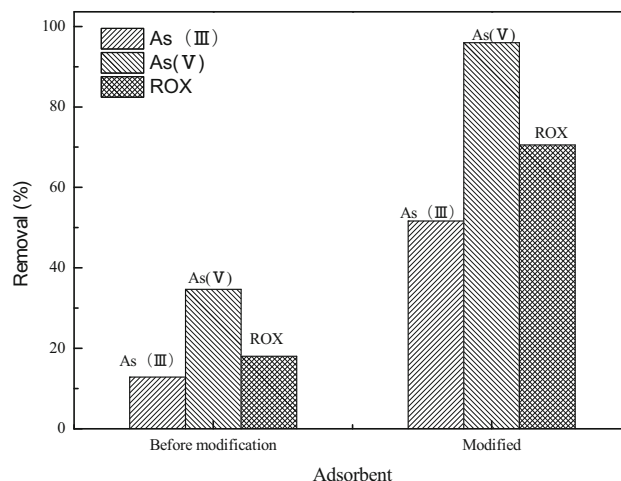


Fig. 5 Adsorbent performance evaluation in a solution at pH 5 using a loading mass of 1 g/L with a ROX and As(III/V) concentration of 1 mg/L

reasons. One is that the formation of Fe–O through the modification of $FeCl_3$ changed the surface structure of the adsorbent, and the modified surface structure enhanced the chemical and/or physical adsorption of the adsorbent. The iron-arsenic co-precipitation (Zhang et al. 2019) that occurred on the MSSB could enhance the type of chemisorption. The second reason may be newly formed C=O/COO groups on the MSSB that played an important role in removing arsenic from the solution (Xie et al. 2019). These results demonstrated the MSSB obtained from SSB was suitable for the simultaneous co-adsorption of ROX and As(III/V).

## 3.3 Effect of adsorbent dosage

The effect of MSSB dose on ROX and As(III/V) was investigated for the removal of arsenic is strongly affected by the dosage of the adsorbent (Wang et al. 2019; Jahangiri
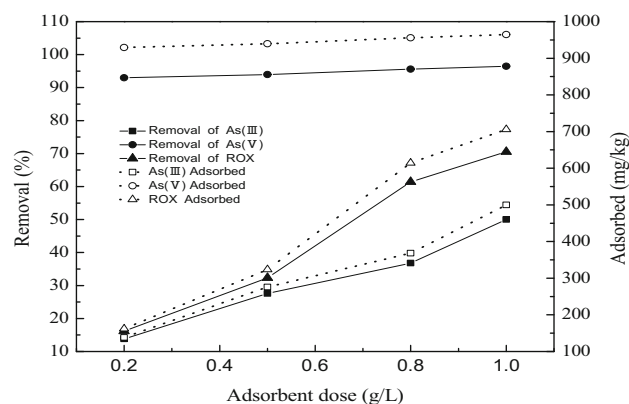


Fig. 6 Effect of the adsorbent dosage on arsenic removal from ROX and As(III/V), respectively, using 1.0 mg/L As at pH 5 and room temperature

et al. 2019). The results were shown in Fig. 6. It can be observed that the removal rate for ROX and As(III) increased rapidly with increasing adsorbent dose. In contrast, the removal rate of As(V) is higher than that of As(III) and remains unchanged substantially as the adsorbent dose increased. The higher removal rate of As(V) likely arises from some preferential adsorption sites that may form some relatively stable complexes and/or compounds (Namasivayam and Senthilkumar 1998; Hu et al. 2012). When the adsorbent dosage was 0.2 g/L, the removal rate of ROX, As(III), and As(V) were 16.20%, 13.81%, and 92.94%, respectively. While the removal rate increased to 70.56%, 50.00%, and 96.47% under the adsorbent dosage of 1.0 g/L. The increase in the removal rate may be largely attributed to more adsorbent supplied more adsorption sites (Gupta et al. 2005; Murugesan et al. 2006). At the MSSB dosage was 1.0 g/L, the adsorption capacities for ROX, As(III), and As(V) were the highest and reached 705.61, 500.00, and 964.68 mg/kg, respectively. The adsorbent dose of 1.0 g/L MSSB was used for the subsequent adsorption tests.

### 3.4 Effect of temperature

Temperature is another significant factor affect adsorption (Yadav et al. 2020). As shown in Fig. 7, the removal rates of three pollutants increased first and then decreased with the increasing temperature. The increase of ionic thermal motion could lead to the decrease of binding stability of the adsorbent with arsenic, resulting in the gradual decrease of adsorption capacity on the adsorbent surface (Fan 2013). When it was 25 °C, the removal rate of ROX, As(III), and As(V) were the highest, reaching 71.57%, 50.79%, and 98.69%, respectively, and the adsorption capacities were 715.7, 507.9, and 998.9 mg/kg, respectively. Compared with previous works (Ebrahimi et al. 2013; Liu 2007), the
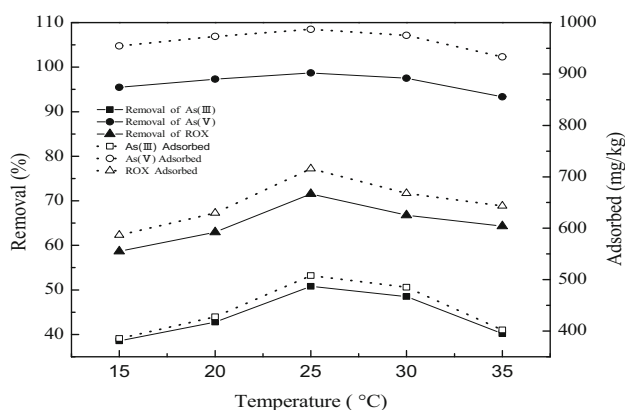
larger adsorption capacity observed in this paper indicates that the method may be suitable to remove the combined pollution of As in the water at 25 °C. Therefore, the temperature of 25 °C was selected, which is more suitable close to practical applications.

### 3.5 Effect of pH

In general, the pH value can affect the adsorption characteristics of the substrate material since it may lead to changes of arsenic in chemical speciation, solubility, and hydrophilicity. In addition, the adsorption of arsenic is severely affected by zero charge ($pH_{pzc}$) of the adsorbent. The $pH_{pzc}$ of the MSSB was estimated according to the method described by Wang et al. (Wang et al. 2019). Figure 8 shows that the $pH_{pzc}$ value of the MSSB is approximately 5.5. The surface charge of the adsorbents is positive at a pH below the $pH_{pzc}$ meanwhile it is negative when the solution pH is above $pH_{pzc}$ (Wang et al. 2019). Considering these two factors, the effect of pH on ROX, As(III) and As(V) removal by MSSB was investigated between 1.0 to 11.0, as shown in Fig. 9.

From Fig. 9, it can be observed that the removal rates of three As species increased first and then decreased with increasing pH values. At pH = 5.0, the removal rates of As(V) and As(III) were the maxima as 99.60% and 62.60%, respectively, and the removal rate of ROX was 71.14%. The uptake of As(V) was remarkably higher than that of ROX and As(III) probably because it was more likely to form stable complexes and/or co-precipitate (Wang et al. 2019). At pH = 5, As(III) and As(V) exist mainly as $H_3AsO_3$ and $H_2AsO_4^-$/ $H_3AsO_4$ (Fan et al. 2013), and the positive-charged surface adsorbent at pH = 5 is beneficial to the adsorption of arsenic in the anion state. At pH = 5.5, the surface of the MSSB
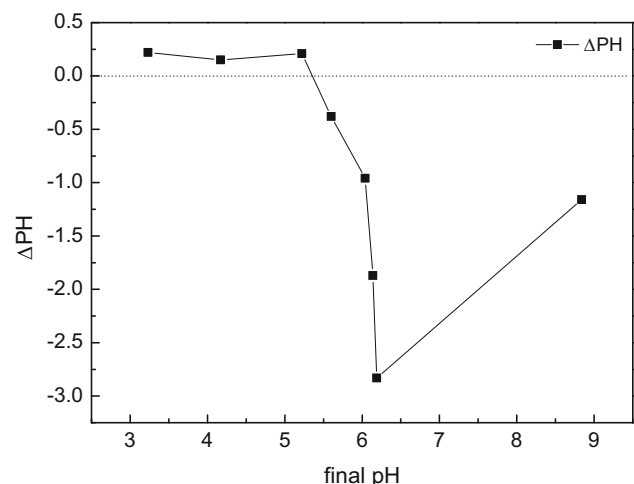


**Fig. 7** Effect of temperature on the removal rates of ROX and As(III/V) by MSSB. The adsorbent of 1 g/L at pH 5 with an As concentration was 1.0 mg/L



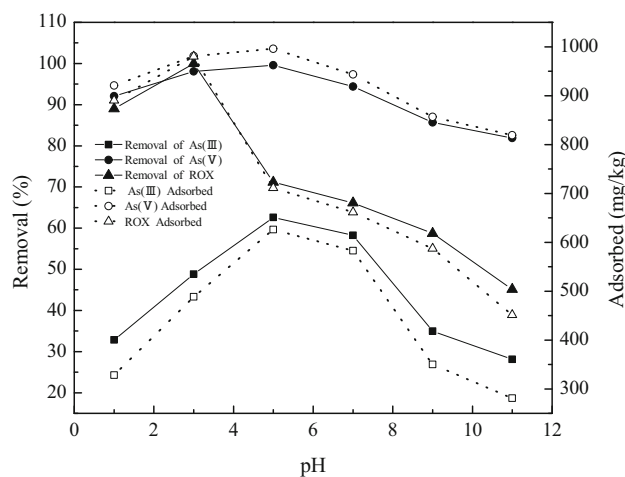**Fig. 8** Point of zero charge of the sorghum straw biochar

**Fig. 9** Effect of pH on the adsorption of ROX and As(III/V) by MSSB. The adsorbent of 1 g/L at room temperature with an As concentration was 1.0 mg/L



**Fig. 10** Relationship between reaction time and removal rate using 1.0 mg/L As at pH 5 with 1.0 g/L MSSB and room temperature

adsorbent was more negatively charged and disfavored the adsorption of the negative arsenic anions species, inducing the decreased removal rate for pH > 5. The removal rate of ROX appeared the maximum at pH = 3.0 and reached close to 100%, which was consistent with the literature (Hu et al. 2012). The increased pH leads to increased ionization and hydrophilicity, which would weaken hydrophobic interactions (Hu et al. 2012) and thus decrease adsorption, causing its lower removal. Therefore, based on these observations the optimal solution at pH = 5 was the default.

### 3.6 Adsorption kinetics

Kinetic is an important criterion for the design of a sorption system because it determines the equilibrium time. To confirm the potential kinetic mechanism of the ROX and As(III/V) sorption on the MSSB, the relationships between time and the removal rate of arsenic were investigated and the result is shown in Fig. 10. In general, it can be observed that the adsorption process of ROX and As(III/V) followed the same trend, including two steps, a relatively rapid adsorption step, and a relatively slow adsorption process. It can be attributed to the presence of two diffusion rates (Wang et al. 2019), external transport at highly accessible surface adsorption sites and intraparticle transport at less accessible internal adsorption sites of the adsorbent. In the case of ROX, the fast removal process appeared within 4 h and the removal rate reached 67.09%. For As(III) and As(V), the fast removal appeared in 12 h and the removal rate reached 46.84% and 86.93%, respectively. In this step, it could due to the different types of arsenic occupied most of the adsorption sites on the surface of the adsorbent,
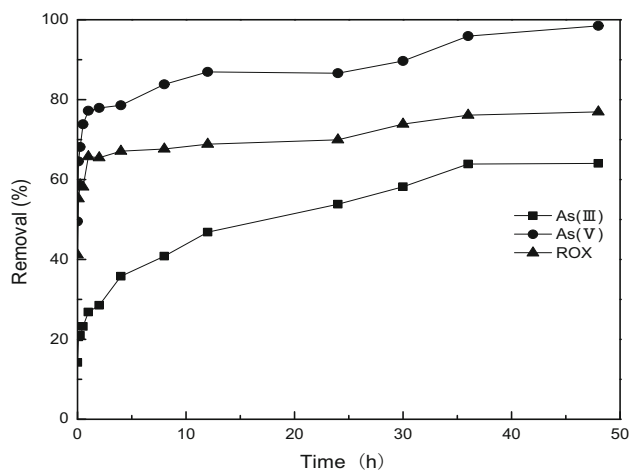
leading to the fast removal rates (Wang et al. 2019). As the reaction time increased and the adsorption sites decreased, the adsorption rates decreased which probably because the adsorption kinetics was dominated by the surface precipitation and intraparticle diffusion at this step. The results were consistent with the previous report (Wang et al. 2019). To ensure complete equilibration, an equilibration time of 48 h was selected for the other batch experiments. As shown in Fig. 10, the system reached equilibrium within 36 h.

To further investigate the adsorption mechanism of the MSSB for ROX and As(III/V), the pseudo-first order and the pseudo-second-order rate equations were fitted to the data. The results are shown in Fig. 11 and the parameters obtained from the kinetic model are listed in Table 2. The results demonstrated the pseudo-second-order rate equation based on chemisorption (Sarntanayoot et al. 2019; Hubbe
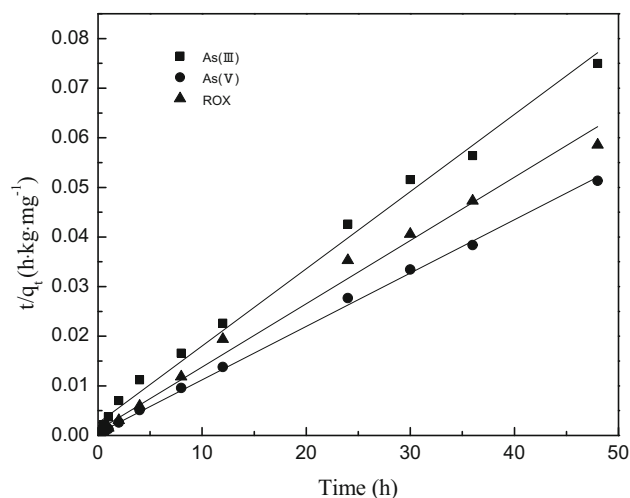


**Fig. 11** The pseudo-second-order rate model of ROX and As(III/V) using 1.0 mg/L As at pH 5 with 1.0 g/L MSSB and room temperature

**Table 2** Kinetic parameters for ROX and As(III/V) by Fe-modified molecular sieves

| Parameters | Pseudo-first-order Kinetics | | | Pseudo-second-order Kinetics | | |
|---|---|---|---|---|---|---|
| | $q_e$ (mg/kg) | $K_1 (h^{-1})$ | $R^2$ | $q_e$ (mg/kg) | $K_2$ (kg/(mg h) | $R^2$ |
| As(III) | 419.02 | 0.07169 | 0.9729 | 641.03 | $9.73 \times 10^{-4}$ | 0.9929 |
| As(V) | 516.39 | 0.1029 | 0.9251 | 925.93 | $2.43 \times 10^{-3}$ | 0.9985 |
| ROX | 467.43 | 0.9181 | 0.9386 | 781.25 | $1.59 \times 10^{-3}$ | 0.9910 |

**Table 3** Isotherms parameters for ROX, As(III) and As(V) adsorption on MSSB

| Parameters | Langmuir model | | | Freundlich model | | | Dubinin-Radushkevich model | | |
|---|---|---|---|---|---|---|---|---|---|
| | $q_m$ (mg/kg) | $K_L$ (L/kg) | $R^2$ | n | $K_F$ | $R^2$ | $\beta$ (mol$^2$ KJ$^{-2}$) | E (KJ/mol) | $R^2$ |
| As(III) | $5.3 \times 10^3$ | $2.14 \times 10^{-4}$ | 0.9935 | 2.9 | 1.6499 | 0.8639 | 0.6596 | 0.87 | 0.9317 |
| As(V) | $2.3 \times 10^4$ | $5.73 \times 10^{-4}$ | 0.9931 | 1.9 | 0.1749 | 0.9560 | 0.0352 | 3.77 | 0.8371 |
| ROX | $1.24 \times 10^4$ | $1.91 \times 10^{-4}$ | 0.9948 | 2.8 | 0.5403 | 0.8899 | 0.1929 | 1.61 | 0.8372 |

et al. 2019), which can describe the experimental kinetics data and the rate-limiting steps in this work. The $q_e$ values of ROX, As(III), and As(V) obtained from the pseudo-second-order equation model respectively were 781.25, 641.03, and 925.93 mg/kg which were in good agreement with results obtained from the batch isotherm work (Table 3).

### 3.7 Adsorption isotherms

To evaluate the adsorption capacities of the MSSB and adsorption mechanism, three isotherms were evaluated (i.e. Langmuir, Freundlich, and Dubinin-Radushkevich) under the optimal adsorption conditions (Uner et al. 2016; Solic et al. 2020; Langmuir 1917). The results are presented in Table 3. According to Table 3, the models of Freundlich and Dubinin-Radushkevich with the lower correlation coefficient were not fitted well with experimental data. Langmuir model displayed a higher determination coefficients ($R^2$) in the range of 0.993 to 1.000, and the Langmuir adsorption isotherm for the adsorption of ROX, As(III) and As(V) is shown in Fig. 12, indicating Langmuir model was the best-fitted model for ROX and As(III/V) adsorption onto MSSB. The monolayer adsorption represented by the Langmuir isotherm model played an important role in the arsenic removal (Feng et al. 2019). The adsorption capacities of ROX, As(III), and As(V) were 12.4, 5.3, and 23 mg/g, respectively. The comparison of previous works (Wang et al. 2019; Ansone et al. 2013; Hu et al. 2012; Lu et al. 2014), indicates that the adsorption capacities of ROX, As(III), and As(V) by MSSB have been improved significantly. Therefore, this method is feasible to simultaneously remove mixed As species, i.e., ROX, As(III), and As(V), in aqueous systems.
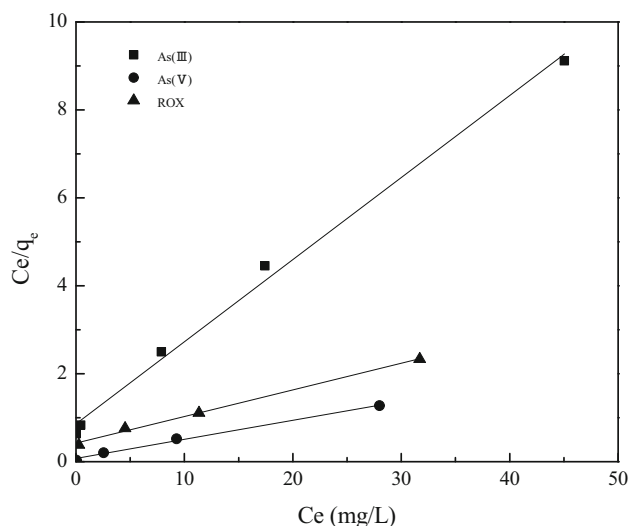


**Fig. 12** Langmuir adsorption isotherm for the adsorption of ROX, As(III) and As(V).Using 1.0 mg/L As at pH 5 with 1.0 g/L MSSB and room temperature

### 4 Conclusion

In this paper, a novel method has been developed for the simultaneous removal of ROX and As (III/V) synthetic aqueous solutions using low-cost sorghum straw biochar modified by FeCl$_3$. The optimal parameters of MSSB for the ROX and As(III/V) removal, such as temperature, adsorbent dose, and pH, have been determined. The adsorption mechanism was described by the pseudo-second-order equation and Langmuir isotherm adsorption. Under the optimal conditions, the excellent adsorption capacities of ROX, As(III), and As(V) have been obtained. The results show that low-cost adsorbent material, MSSB

possesses a good adsorption effect on arsenic contaminations and great potential for environmental restoration applications.

## References

Ali W, Rasool A, Junaid M, Zhang H (2019) A comprehensive review on current status, mechanism, and possible sources of arsenic contamination in groundwater: a global perspective with prominence of Pakistan scenario. Environ Geochem Health 41(2):737–760

Ansone L, Klavins M, Viksna A (2013) Arsenic removal using natural biomaterial-based sorbents. Environ Geochem Health 35(5):633–642

Asere TG, Stevens CV, Du Laing G (2019) Use of (modified) natural adsorbents for arsenic remediation: a review. Sci Total Environ 676:706–720

Calugaru IL, Neculita CM, Genty T, Zagury GJ (2019) Removal efficiency of As(V) and Sb(III) in contaminated neutral drainage by Fe-loaded biochar. Environ Sci Pollut Res 26(9):9322–9332

Chandra V, Park J, Chun YS, Lee JW, Hwang I, Kim KS (2010) Water-dispersible magnetite-reduced graphene oxide composites for arsenic removal. ACS Nano 4(7):3979–3986

Cheraghi M, Lorestani B, Merrikhpour H, Mosaed HP (2014) Assessment efficiency of tea wastes in arsenic removal from aqueous solution. Desalin Water Treat 52:7235–7240

Danish MI, Qazi IA, Zeb A, Habib A, Awan MA, Khan Z (2013) Arsenic removal from aqueous solution using pure and metal-doped titania nanoparticles coated on glass beads: adsorption and column studies. J Nanomater 2013:4979–4984

Dixit S, Hering JG (2003) Comparison of arsenic(V) and arsenic(III) sorption onto iron oxide minerals: implications for arsenic mobility. Environ Sci Technol 37(18):4182–4189

Dupont L, Jolly G, Aplincourt M (2007) Arsenic adsorption on lignocellulosic substrate loaded with ferric ion. Environ Chem Lett 5(3):125–129

Ebrahimi R, Maleki A, Shahmoradi B, Daraei H, Mahvi AH, Barati AH, Eslami A (2013) Elimination of arsenic contamination from water using chemically modified wheat straw. Desalin Water Treat 51:2306–2316

Eisler R (2004) Arsenic hazards to humans, plants, and animals from gold mining. Rev Environ Contam Toxicol 180:133–165

Fan W (2013) Study on arsenic adsorption performance by sulfhydryl silane modified oxidation graphite. Environ Chem 32:810–818

Feng Z, Chen N, Feng C, Fan C, Wang H, Deng Y, Gao Y (2019) Roles of functional groups and irons on bromate removal by FeCl3 modified porous carbon. Appl Surf Sci 488:681–687

Frensemeier LM, Buter L, Vogel M, Karst U (2017) Investigation of the oxidative transformation of roxarsone by electrochemistry coupled to hydrophilic interaction liquid chromatography/mass spectrometry. J Anal At Spectrom 32(1):153–161

Fu W, Lu D, Yao H, Yuan S, Wang W, Gong M, Hu Z (2020) Simultaneous roxarsone photocatalytic degradation and arsenic adsorption removal by TiO2/FeOOH hybrid. Environ Sci Pollut Res 27:1–9

Gomez MA, Berre JL, Assaaoudi H, Demopoulos GP (2011) Raman spectroscopic study of the hydrogen and arsenate bonding environment in isostructural synthetic arsenates of the variscite group—$M^{3+}$ AsO4·2H2O ($M^{3+}$ = Fe, Al, In and Ga): implications for arsenic release in water. J Raman Spectrosc 42(1):62–71

Guo S, Feng B, Zhang H (2011) Simultaneous determination of trace arsenic and antimony in Fomes Officinalis Ames with hydride generation atomic fluorescence spectrometry. J Fluoresc 21(3):1281–1284

Gupta VK, Saini VK, Jain N (2005) Adsorption of As(III) from aqueous solutions by iron oxide-coated sand. J Colloid Interface Sci 288(1):55–60

Guzmán-Fierro V, Moraga R, Leon C, Campos VL, Smith CT, Mondaca MA (2015) Isolation and characterization of an aerobic bacterial consortium able to degrade roxarsone. Int J Environ Sci Technol 12(4):1353–1362

Hao L, Liu M, Wang N, Li G (2018) A critical review on arsenic removal from water using iron-based adsorbents. RSC Adv 8(69):39545–39560

Hossain I, Anjum N, Tasnim T (2016) Removal of arsenic from contaminated water utilizing tea waste. Int J Environ Sci Technol 13(3):843–848

Hu J, Tong Z, Hu Z, Chen G, Chen T (2012) Adsorption of roxarsone from aqueous solution by multi-walled carbon nanotubes. J Colloid Interface Sci 377(1):355–361

Hubbe MA, Azizian S, Douven S (2019) Implications of apparent pseudo-second-order adsorption kinetics onto cellulosic materials: a review. BioResources 14(3):7582–7626

Iglesias O, De Dios MA, Pazos M, Sanroman MA (2013) Using iron-loaded sepiolite obtained by adsorption as a catalyst in the electro-Fenton oxidation of Reactive Black 5. Environ Sci Pollut Res 20(9):5983–5993

Jahangiri K, Yousefi N, Ghadiri SK, Fekri R, Bagheri A, Talebi SS (2019) Enhancement adsorption of hexavalent chromium onto modified fly ash from aqueous solution; optimization; isotherm, kinetic and thermodynamic study. J Dispersion Sci Technol 40(8):1147–1158

Ji Y, Shi Y, Kong D, Lu J (2016) Degradation of roxarsone in a sulfate radical mediated oxidation process and formation of polynitrated by-products. RSC Adv 6(85):82040–82048

Kim J, Benjamin MM (2004) Modeling a novel ion exchange process for arsenic and nitrate removal. Water Res 38(8):2053–2062

Kumari P, Sharma P, Srivastava S, Srivastava MM (2005) Arsenic removal from the aqueous system using plant biomass: a bioremedial approach. J Ind Microbiol Biotechnol 32(11):521–526

Langmuir I (1917) The constitution and fundamental properties of solids and liquids. J Frankl Inst Eng Appl Math 183(1):102–105

Lee KE, Gomez MA, Elouatik S, Demopoulos GP (2010) Further understanding of the adsorption mechanism of N719 sensitizer on anatase TiO2 films for DSSC applications using vibrational spectroscopy and confocal raman imaging. Langmuir 26(12):9575–9583

Li B, Zhu X, Hu K, Li Y, Feng J, Shi J, Gu J (2016) Defect creation in metal-organic frameworks for rapid and controllable decontamination of roxarsone from aqueous solution. J Hazard Mater 302:57–64

Lin X, Wang L, Jiang S, Cui L, Wu G (2019) Iron-doped chitosan microsphere for As(III) adsorption in aqueous solution: kinetic, isotherm and thermodynamic studies. Korean J Chem Eng 36(7):1102–1114

Liu ZP (2007) The sorption characteristics of roxarsone in soils. J Agro Environ Sci 06:2075–2079

Lu D, Ji F, Wang W, Yuan S, Hu Z, Chen T (2014) Adsorption and photocatalytic decomposition of roxarsone by $TiO_2$ and its mechanism. Environ Sci Pollut Res 21(13):8025–8035

Ma J, Zhuang Y, Yu F (2015) Equilibrium, kinetic and thermodynamic adsorption studies of organic pollutants from aqueous solution onto CNT/C@Fe/chitosan composites. New J Chem 39(12):9299–9305

Mahaninia MH, Wilson LD (2017) A kinetic uptake study of roxarsone using cross-linked chitosan beads. Ind Eng Chem Res 56(7):1704–1712

Mohanty D (2017) Conventional as well as emerging arsenic removal technologies—a critical review. Water Air Soil Pollut 228(10):1–21

Murugesan GS, Sathishkumar M, Swaminathan K (2006) Arsenic removal from groundwater by pretreated waste tea fungal biomass. Biores Technol 97(3):483–487

Namasivayam C, Senthilkumar S (1998) Removal of arsenic(V) from aqueous solution using industrial solid waste: Adsorption rates and equilibrium studies. Ind Eng Chem Res 37(12):4816–4822

Ng K, Ujang Z, Leclech P (2004) Arsenic removal technologies for drinking water treatment. Environ Sci Biotechnol 3(1):43–53

Ocinski D, Jacukowiczsobala I, Kociolekbalawejder E (2016) Alginate beads containing water treatment residuals for arsenic removal from water—formation and adsorption studies. Environ Sci Pollut Res 23(24):24527–24539

Pal P, Ahammad SZ, Pattanayak A, Bhattacharya P (2007) Removal of arsenic from drinking water by chemical precipitation - a modeling and simulation study of the physical-chemical processes. Water Environ Res 79(4):357–366

Philippova O, Barabanova A, Molchanov V, Khokhlov A (2011) Magnetic polymer beads: recent trends and developments in synthetic design and applications. Eur Polymer J 47(4):542–559

Pokhrel D, Viraraghavan T (2006) Arsenic removal from aqueous solution by iron oxide-coated fungal biomass: a factorial design analysis. Water Air Soil Pollut 173(1):195–208

Sarntanayoot P, Fuangswasdi S, Imyim A (2019) Iron nanoparticle-modified water treatment residues for adsorption of As(III) and As(V) and their cement-based solidification/stabilization. Int J Environ Sci Technol 16(8):4285–4292

Seidel A, Waypa JJ, Elimelech M (2001) Role of charge (Donnan) exclusion in removal of arsenic from water by a negatively charged porous nanofiltration membrane. Environ Eng Sci 18(2):105–113

Setyono D, Valiyaveettil S (2014) Multi-metal oxide incorporated microcapsules for efficient As(III) and As(V) removal from water. RSC Adv 4(95):53365–53373

Solesardans M, Gamisans X, Dorado AD, Laoluque C (2016) Exploring arsenic adsorption at low concentration onto modified leonardite. Water Air Soil Pollut 227(4):128

Solic M, Maletic S, Isakovski MK, Nikic J, Watson M, Konya Z, Trickovic J (2020) Comparing the adsorption performance of multiwalled carbon nanotubes oxidized by varying degrees for removal of low levels of copper, nickel and chromium(VI) from aqueous solutions. Water 12(3):723

Su H, Ye Z, Hmidi N, Subramanian R (2017) Carbon nanosphere–iron oxide nanocomposites as high-capacity adsorbents for arsenic removal. RSC Adv 7(57):36138–36148

Tian C, Zhao J, Zhang J, Chu S, Dang Z, Lin Z et al (2017) Enhanced removal of roxarsone by fe3o4@3d graphene nanocomposites: synergistic adsorption and mechanism. Nano, Environmental Science, p 4

Tian Y, Wu M, Lin X, Huang P, Huang Y (2011) Synthesis of magnetic wheat straw for arsenic adsorption. J Hazard Mater 193:10–16

Uner O, Gecgel U, Bayrak Y (2016) Adsorption of methylene blue by an efficient activated carbon prepared from citrullus lanatus rind: kinetic, isotherm, thermodynamic, and mechanism analysis. Water Air Soil Pollut 227(7):247

Ustinov EA, Do DD (2002) Adsorption in slit-like pores of activated carbons: improvement of the Horvath and Kawazoe method. Langmuir 18(12):4637–4647

Wang Y, Wang S, Zhang G, Wang X, Zang S, Jia Y (2019) Removal of As(V) and As(III) species from wastewater by adsorption on coal fly ash. Desalin Water Treat 151:242–250

WHO (2001). http://www.who.int/inf/en/index-pr.2002.html

Xie X, Zhao W, Hu Y, Xu X, Cheng H (2019) Permanganate oxidation and ferric ion precipitation ($KMnO_4$-Fe(III)) process for treating phenylarsenic compounds. Chem Eng J 357:600–610

Yadav MK, Gupta AK, Ghosal PS, Mukherjee A (2020) Remediation of carcinogenic arsenic by pyroaurite-based green adsorbent: isotherm, kinetic, mechanistic study, and applicability in real-life groundwater. Environ Sci Pollut Res 27:24982–24998

Yang X, Xu G, Yu H, Zhang Z (2016) Preparation of ferric-activated sludge-based adsorbent from biological sludge for tetracycline removal. Biores Technol 211:566–573

Yasinta J, Emery DV, Daniel M (2018) A comparative study on removal of hazardous anions from water by adsorption: a review. Int J Chem Eng 2018:1–21

Yu X, Han X, Chang C, Hu Y, Xu C, Fang S (2020) Corncob-derived activated carbon for roxarsone removal from aqueous solution: isotherms, kinetics, and mechanism. Environ Sci Pollut Res 27(13):15785–15797

Zhang G, Yuan Z, Lei L, Lin J, Wang X, Wang S, Jia Y (2019) Arsenic redistribution and transformation during Fe(II)-catalyzed recrystallization of As-adsorbed ferrihydrite under anaerobic conditions. Chem Geol 525:380–389

Zhang Y, Liu J (2019) Density functional theory study of arsenic adsorption on the Fe2O3 (001) surface. Energy Fuels 33(2):1414–1421

Zhu S, Zhao J, Zhao N, Yang X, Chen C, Shang J (2020) Goethite modified biochar as a multifunctional amendment for cationic Cd(II), anionic As(III), roxarsone, and phosphorus in soil and water. J Clean Prod 247:119579